

REPORT DOCUMENTATION PAGE

Form Approved
OMB No. 0704-0188

Public reporting burden for this collection of information is estimated to average 1 hour per response, including the time for reviewing instructions, searching existing data sources, gathering and maintaining the data needed, and completing and reviewing this collection of information. Send comments regarding this burden estimate or any other aspect of this collection of information, including suggestions for reducing this burden to Department of Defense, Washington Headquarters Services, Directorate for Information Operations and Reports (0704-0188), 1215 Jefferson Davis Highway, Suite 1204, Arlington, VA 22202-4302. Respondents should be aware that notwithstanding any other provision of law, no person shall be subject to any penalty for failing to comply with a collection of information if it does not display a currently valid OMB control number. PLEASE DO NOT RETURN YOUR FORM TO THE ABOVE ADDRESS.

1. REPORT DATE (DD-MM-YYYY) 31/07/02	2. REPORT TYPE FINAL TECHNICAL	3. DATES COVERED (From - To) 2/1/99 - 11/30/01		
4. TITLE AND SUBTITLE Corrosion-Induced Multiple Site Damage		5a. CONTRACT NUMBER		
		5b. GRANT NUMBER F49620-99-1-0136		
		5c. PROGRAM ELEMENT NUMBER		
6. AUTHOR(S) Karl Sieradzki Dusan Krajcinovic		5d. PROJECT NUMBER		
		5e. TASK NUMBER		
		5f. WORK UNIT NUMBER		
7. PERFORMING ORGANIZATION NAME(S) AND ADDRESS(ES) Arizona State University Dept. of Mechanical and Aerospace Engineering Tempe, Arizona 85287-6106		8. PERFORMING ORGANIZATION REPORT NUMBER XAA 0060/TE		
9. SPONSORING / MONITORING AGENCY NAME(S) AND ADDRESS(ES) Air Force Office of Walter F. Jones Scientific Research, AFOSR/NA 801 North Randolph Street Room 732 Arlington, VA 22203-1977		10. SPONSOR/MONITOR'S ACRONYM(S) AFOSR		
		11. SPONSOR/MONITOR'S REPORT NUMBER(S)		
12. DISTRIBUTION / AVAILABILITY STATEMENT Unlimited				
13. SUPPLEMENTARY NOTES				
<p style="text-align: right;">20020815 092</p> <p>14. ABSTRACT This research focuses on three key issues related to the nucleation and growth of corrosion fatigue cracks in fuselage fastener holes. (1) The identification of the precise mechanisms responsible for corrosion damage in Al alloy 2024-T3 in the bare, clad, and painted condition. (2) The transitional behavior from corrosion damage to fatigue crack growth nucleation and subsequent short crack growth, and (3) a real-time statistically based model of damage evolution in a structural element.</p> <p>Another aspect of the multiple site damage (MSD) problem that we address is related to the striking observation that there is relative size uniformity of the fatigue cracks from rivet to rivet. The transition from uniform damage (mean field behavior) to that dominated by the propagation of the largest crack in the system is a key aspect of lap joint failure. Often, the onset of such a transition is determined by monitoring the changes occurring in a suitable <i>order parameter</i>. Several possible scenarios for this behavior are explored including chemical short crack effects, and local load redistribution processes similar to what occurs during damage evolution in parallel bar models.</p> <p>15. SUBJECT TERMS Corrosion fatigue, Multiple site damage, order parameter, parallel bar model</p>				
16. SECURITY CLASSIFICATION OF: a. REPORT		17. LIMITATION OF ABSTRACT c. THIS PAGE	18. NUMBER OF PAGES 11	19a. NAME OF RESPONSIBLE PERSON Karl Sieradzki
				19b. TELEPHONE NUMBER (include area code) (480) 965-8990

Corrosion-Induced Multiple Site Damage

THE FOLLOWING WAS ORIGINALLY SUBMITTED IN SEPTEMBER 2001 AND WAS
MEANT TO SERVE AS A FINAL REPORT

AFOSR Aging Aircraft Final Program Report 2001

K. Sieradzki* and D. Krajcinovic

Department of Mechanical and Aerospace Engineering
Arizona State University
Tempe, Arizona 85287-6106

*K. Sieradzki, tel: 480-965-9100, fax: 480-965-1384, email: karl@icarus.eas.asu.edu

1. Executive Summary (Introduction)

Herein we describe research done over the past year on our AFOSR program, "Corrosion-Induced Multiple Site Damage". This research focuses on three key issues related to the nucleation and growth of corrosion fatigue cracks in fuselage fastener holes. (1) The identification of the precise mechanisms responsible for corrosion damage in Al alloy 2024-T3 in the bare, clad, and painted condition. (2) The transitional behavior from corrosion damage to fatigue crack growth nucleation and subsequent short crack growth, and (3) a real-time statistically based model of damage evolution in a structural element.

Another aspect of the multiple site damage (MSD) problem that we address is related to the striking observation that that there is relative size uniformity of the fatigue cracks from rivet to rivet. The transition from uniform damage (mean field behavior) to that dominated by the propagation of the largest crack in the system is a key aspect of lap joint failure. Often, the onset of such a transition is determined by monitoring the changes occurring in a suitable *order parameter*. We propose to explore several possible scenarios for this behavior including chemical short crack effects, and local load redistribution processes similar to what occurs during damage evolution in parallel bar models. As described in this report, the major results of our work over the past year are the following.

- statistical characterizations second phase particles in Al alloy 2024-T3 in order to identify the nature of incipient fatigue crack nuclei
- development of system and initiation of measurement of the kinetics of corrosion induced stress buildup from processes such as pillowowing
- A modeling study of length scale independent statistical scaling of distributions associated with corrosion induced damage.

1.2 Graduate students supported by this program

Lei Tang (100%)

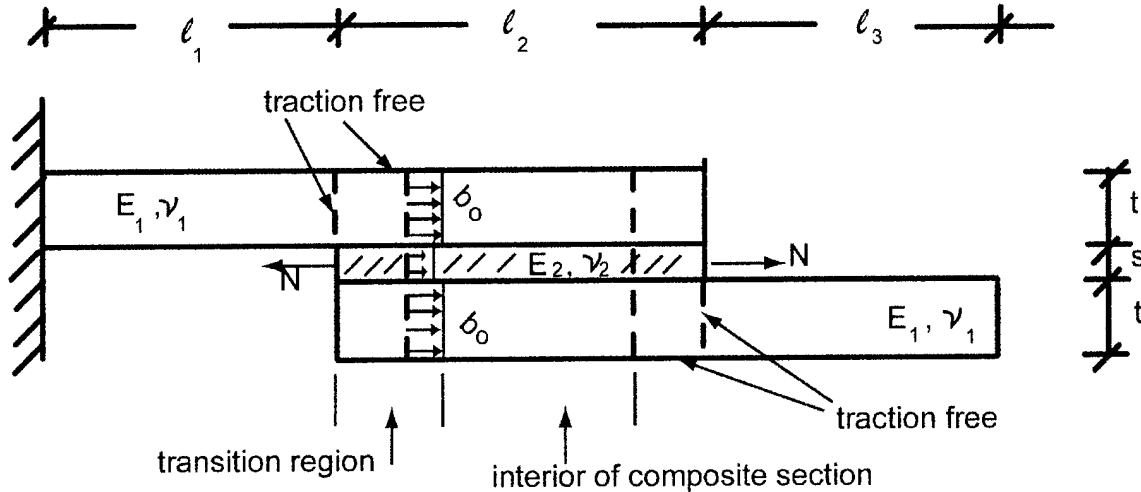
Ratsko Vasill (100%)

1.3 Major Accomplishments

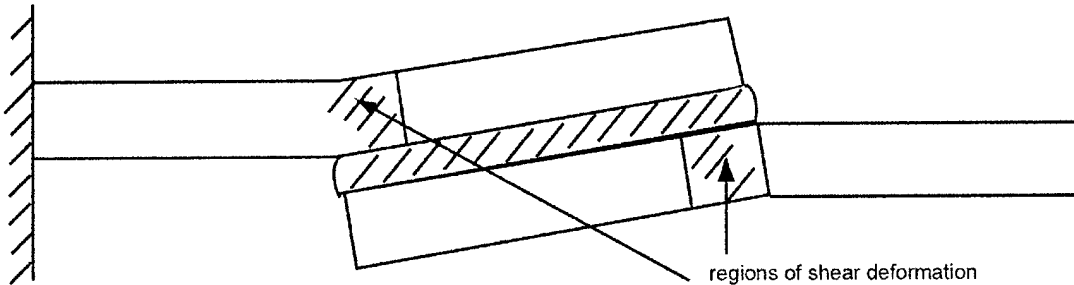
We have completed what we believe to be the most comprehensive study to date measuring the statistics of corrosion damage on Al Alloy 2024-T3 in the RD, ST, and LT orientations as a function of time and sample size.

2.0 Modeling – Deformation induced by pillowing

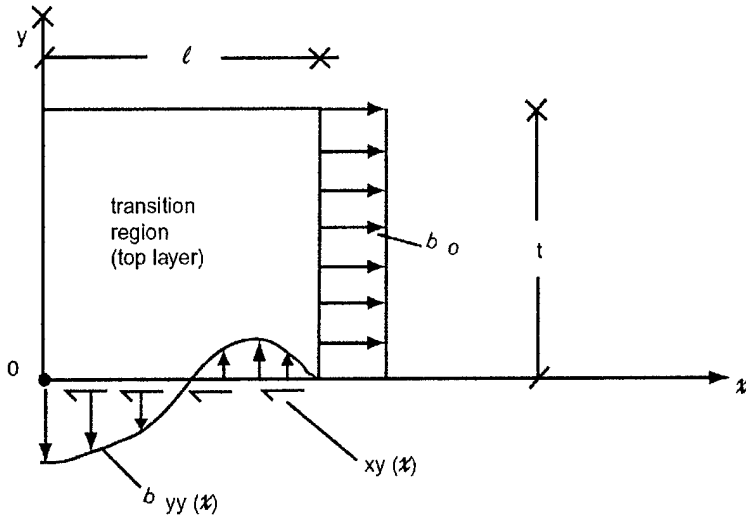
In our analysis of pillowing stresses that evolve during experiments, it has become clear that there is no bending induced in the composite cantilever specimen. Consider the figure below showing the specimen used in experiments.



Here E_1 and v_1 correspond to the Young's modulus and Poisson's ratio of the Al 2024-T3, E_2 and v_2 are the corresponding quantities of the corrosion product which produces an eigenstrain, ϵ^* . The transformation strain, ϵ^* results from the corrosion product build-up and produces deformations indicated in the sketch below.



All of the deformation is localized to the shear regions indicated in the diagram above. A close-up of the shear deformation region on the left side of this figure is shown below.



The transition region is subjected to 3 loading conditions:

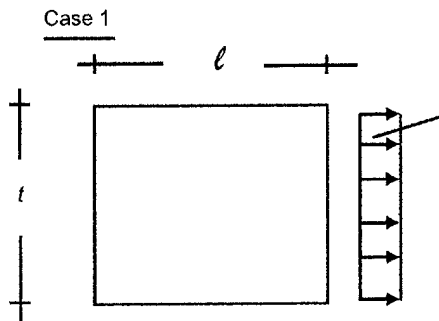
- (1) $\sigma_o = \text{constant on } x = l, 0 \leq y \leq t$
- (2) $\tau_{xy}(x)$ – the profile of which is unknown on $y = 0, 0 \leq x \leq l$
- (3) $\sigma_{yy}(x)$ - the profile of which is unknown on $y = 0, 0 \leq x \leq l$

Consideration of static equilibrium leads to the following relations between these quantities.

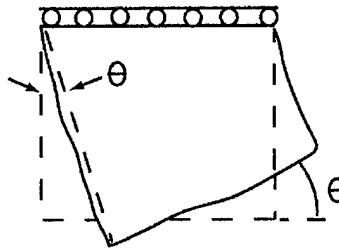
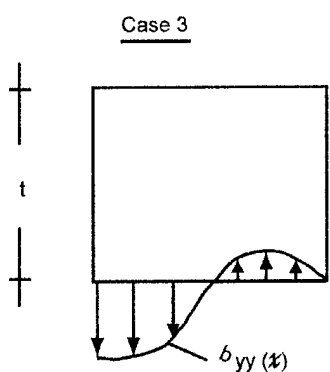
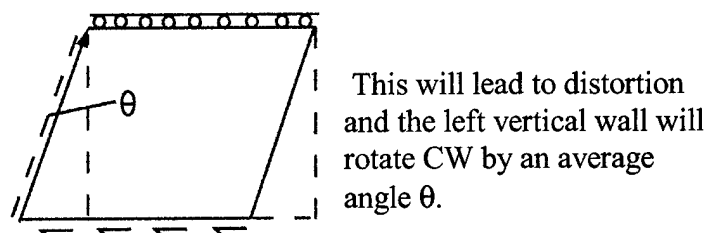
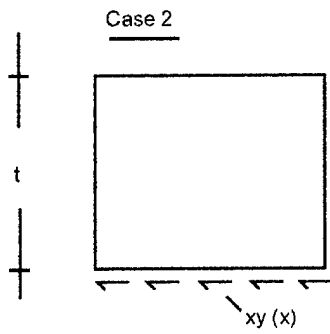
$$\sum F_x = 0, \quad \int_0^l \tau_{xy}(x) dx = \sigma_o t, \text{ and}$$

$$\sum M_o = 0, \quad \int_0^l \sigma_{yy}(x) x dx = \frac{1}{2} \sigma_o t^2.$$

We can determine the combined effects of loading using linear superposition.



This case causes no rotation of the left wall, (i.e., $x = 0, 0 \leq y \leq t$).



The angle θ can be estimated by detailed examination of case 2 or 3. In the shear loading case assuming the following linear form for $\tau_{xy}(x)$, $\tau_{xy}(x) = \frac{\tau_o}{t}(y - y_0)$, one can show that $\theta = \frac{\tau_o}{2G}$, where G is the shear modulus. Finally, the unknown quantity τ_o can be related to the transformation strain ϵ^* ,

$$\theta = (1 + v_1) \frac{t}{l} \frac{\epsilon^*}{1 + 2 \frac{t}{s} \frac{E_1}{E_2} \frac{1 - v_2^2}{1 - v_1^2}}.$$

The main aspects of this analysis have been confirmed with finite element methods. Measurement of the angle θ allows for the determination of the eigenstrain.

3.0 Statistics of pitting damage in Al alloy 2024-T3

Over the past year we have performed detailed statistical studies of corrosion induced pitting damage on Al alloy 2024-T3. RD and LT surfaces of Al alloy 2024-T3 were mechanically polished to a $0.05 \mu\text{m}$ finish in the and exposed to the following solutions, {concentrations indicated mM}:

- Al(OH)_3 {1.42}, Ca(OH)_2 {1.97}, MgCl_2 {0.11}, MgSO_4 {2.40}, NaNO_3 {0.108}, NaF {0.047}, resulting in a $\text{pH} \sim 10.5$ solution
- Cl^- {20}, NO_3^- {4}, bicarbonate {4}, F^- {2} adjusted to $\text{pH} 9$.
- 0.5M Cl^-

Prior to and following exposure in an electrolyte for prescribed times, atomic force microscopy and high resolution scanning electron microscopy were used to characterize the size distribution of second phase particles and holes on the surface of the alloy. Exposure times of 0.5, 2.5, 6.0, 12, 31, 125, 200 and 318 hours were used for samples ranging in aerial size from $10^2 - 10^8 \mu\text{m}^2$. At least six samples of each size and exposure time are currently being examined.

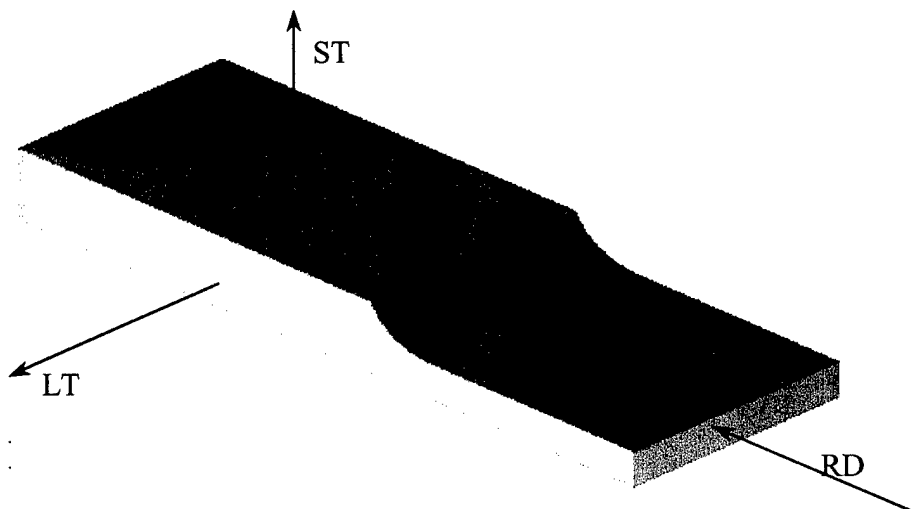


Fig. 1. The three surfaces studied surfaces on Al 2024-T3.

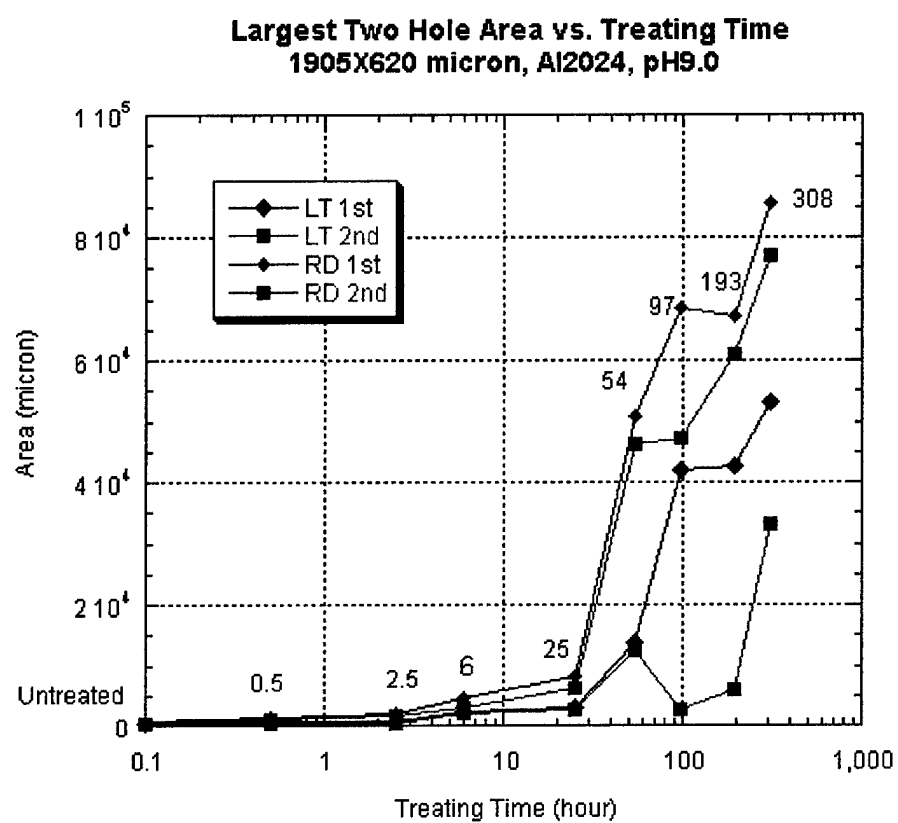


Fig.2. The first and second largest hole area of RD and LT surface vs. treating time with image size 1905X620.

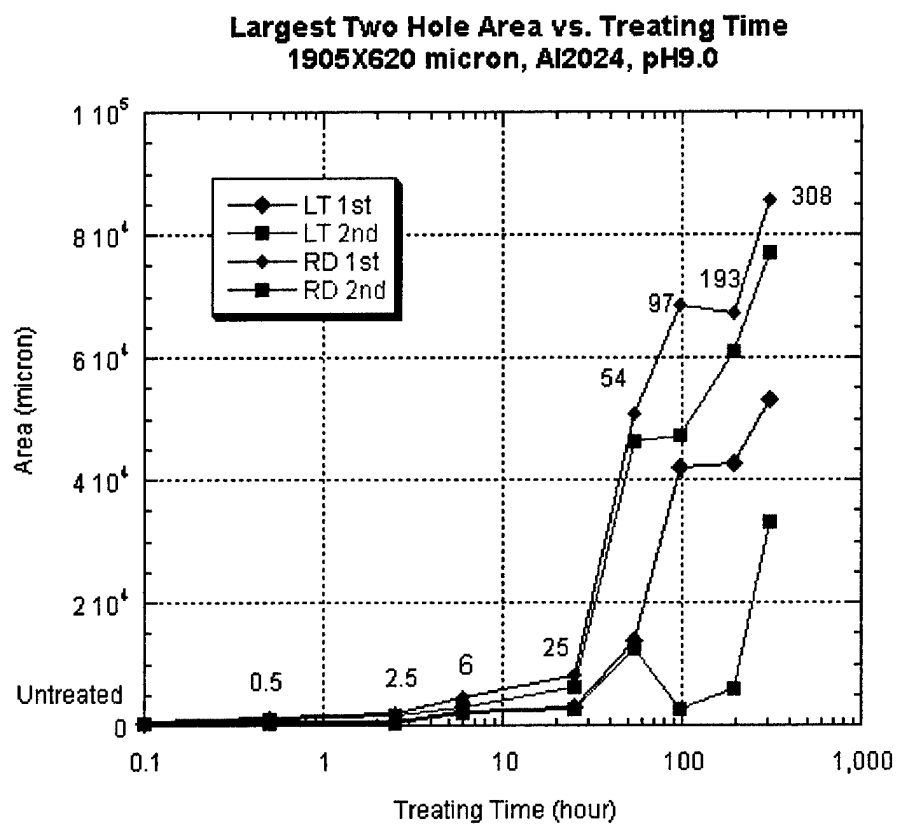


Fig.3. The first and second largest hole area of RD and LT surface vs. treating time with image size 1905X620.

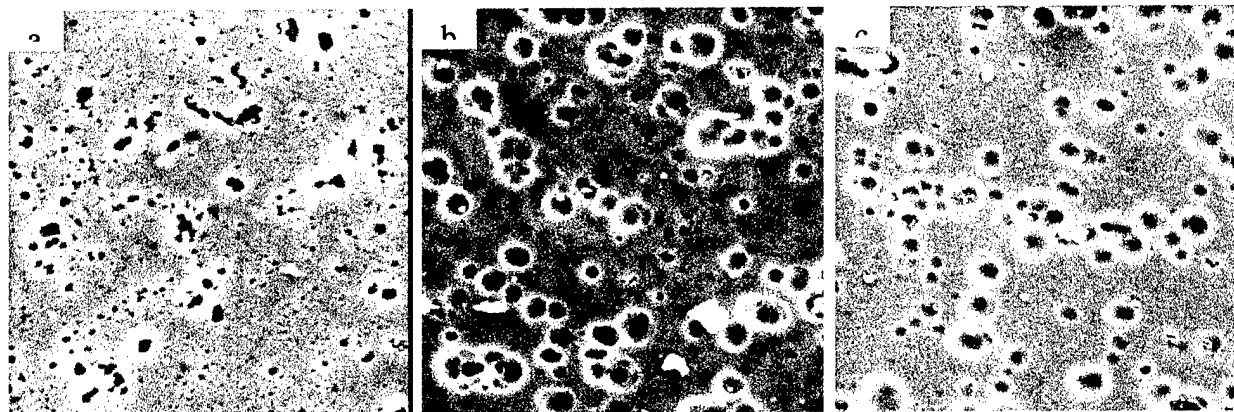


Fig. 4. The 108X108 (micron) SEM image for ST (a), LT (b) and RD (c) surface of Al2024 treated 308 hrs, pH9.0.

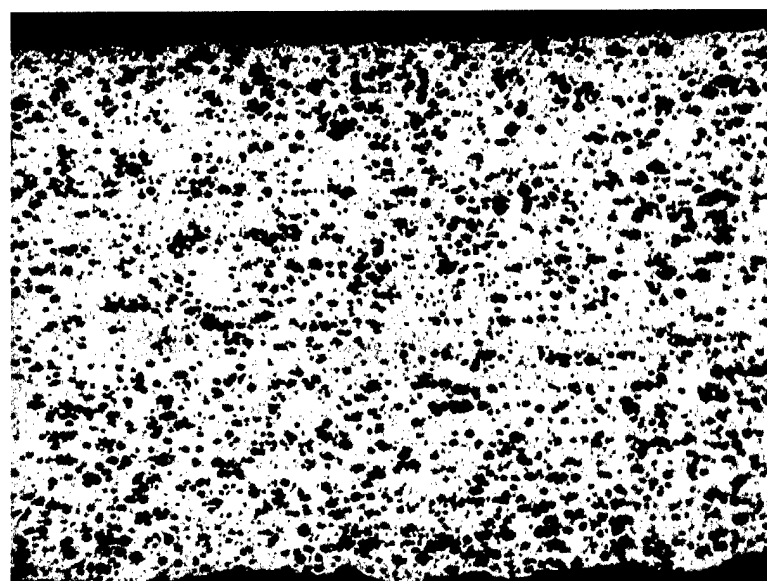
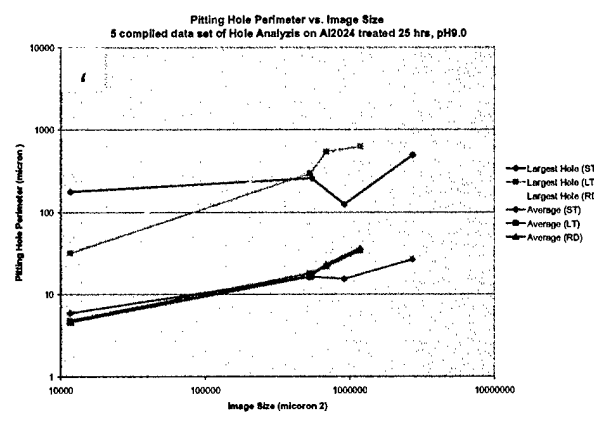
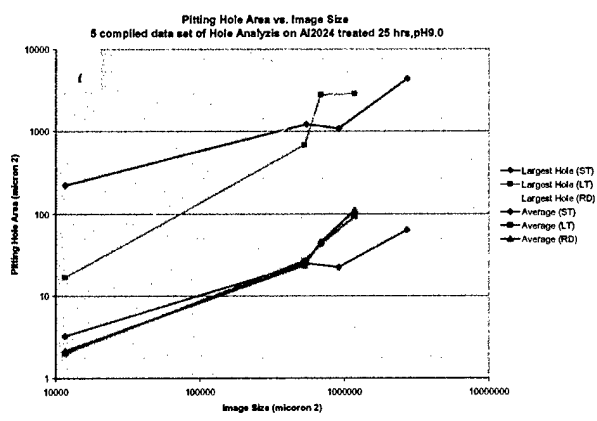
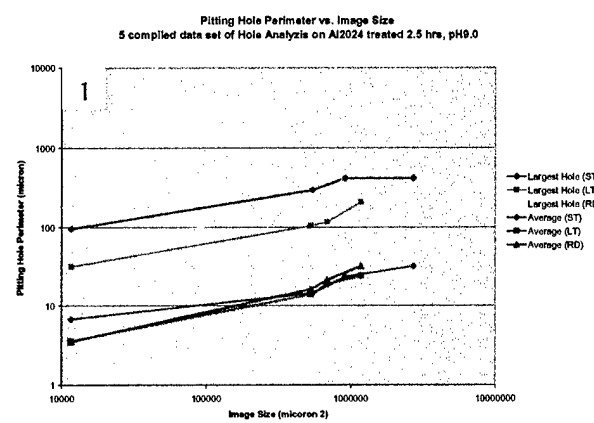
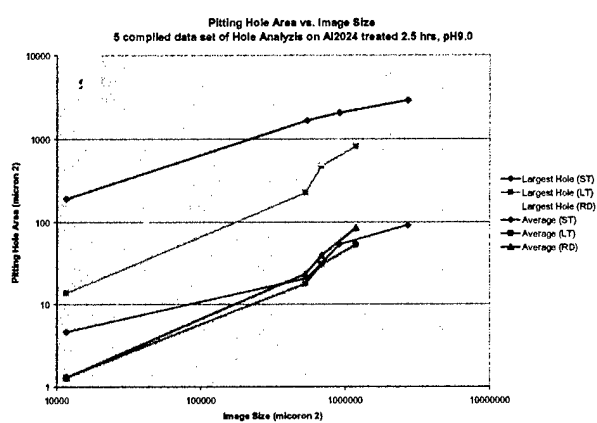


Fig. 5. The optical image of RD surface treated 308hrs. Image Size 825X620 (micron).



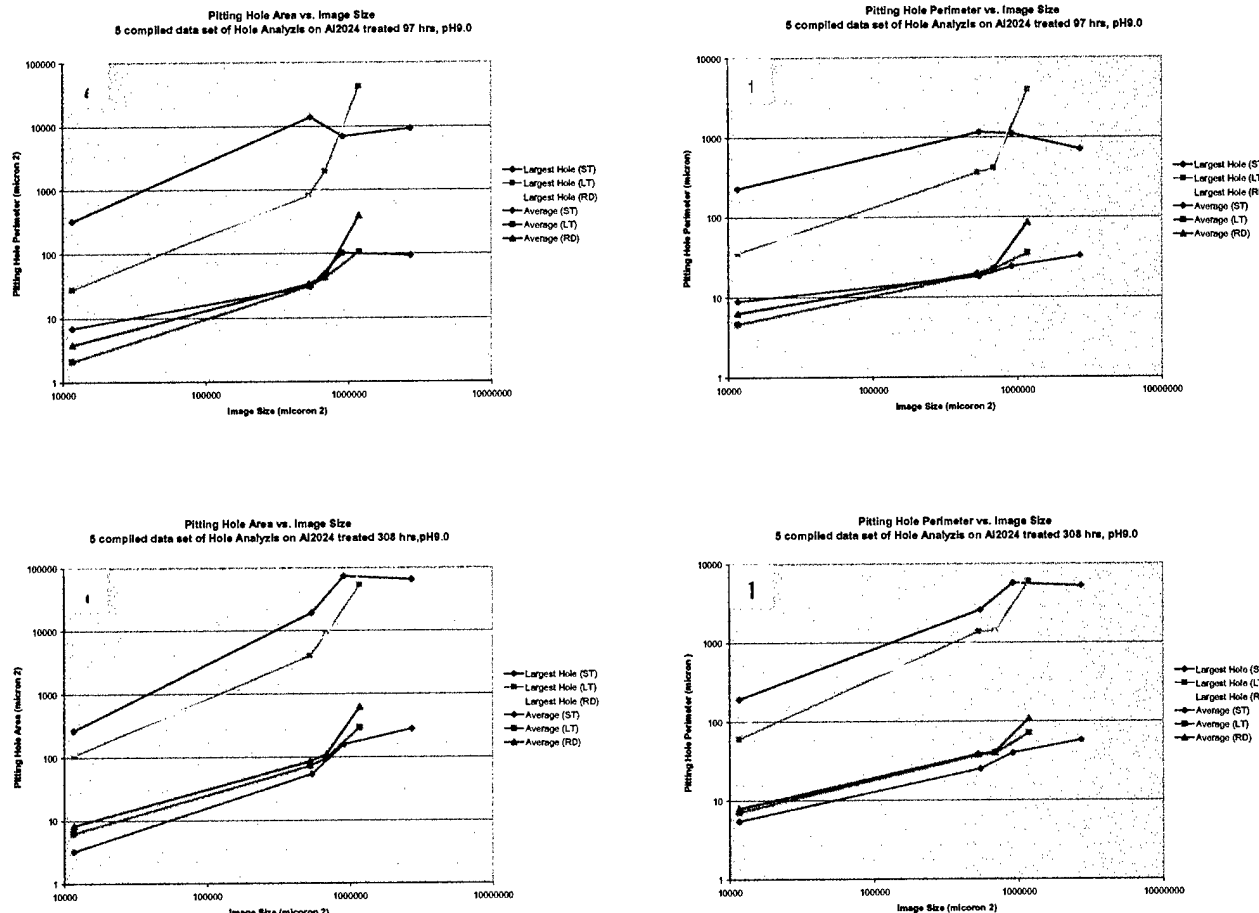


Fig.6. The area and perimeter of pits vs. image size for treating time 2.5 hrs (a, b), 25 hrs (c, d), 97 hrs (e, f) and 308 hrs (g, h).

Summary of results

1. At the beginning, the area of pitting holes slightly increase with time. After a certain time (ca. 25 ~97 hrs), the growth rate is sharp enhanced and at least logarithmic proportional to the treating time, as shown in Fig.2.
2. The RD surface is more reactive than the LT surface, while both of them are easier to be corroded than the ST surface. For a long treating time, for example 308 hrs, the RD and LT surfaces are almost totally damaged by the pitting corrosion, but the ST surface is much less corroded than the other two as shown in Fig.3. This phenomenon indicates that the RD and LT surfaces run a more important role in Multiple Site Damage (MSD) in airframe aluminum alloys than ST face.
3. The pitting holes grow independently at the beginning and joint each other when they meet, as shown in Fig. 3b. Most of the pitting holes show disk shape before merging. This can explain the similar shape of the largest and average curve between pitting hole area and perimeter, showing in Fig.4.
4. The parameters of pitting hole also increase with the image size in a approximately logarithmic pattern, indicating in Fig.4.
5. When the treating time is long, there are tons of tiny pits on the sample surface which can not be observed in detail even by SEM. As shown in Fig.3b, the cloudy parts within existed pitting holes are these micro pits. This phenomenon indicates these surfaces are already corroded even though these tiny pits can not be counted in our data. They are believed to be metastable pits and enhance the later corrosion.
6. The edge is more active than the center of the surface, showing in Fig 5.